Review and Declaration

This thesis has been accepted by the first reviewer of the master thesis.

Karlsruhe, TBD

_____
Prof. Dr. Ralph Engel

I declare that the work in this thesis was carried out in accordance with the requirements of the university's regulations and that it has not been submitted for any other academic award. Except where indicated by specific reference in the text, the work is the candidate's own work. Work done in collaboration with, or with the assistance of, others is indicated as such.

Karlsruhe, TBD

_____
Paul Filip

Contents

1 Physics of cosmic rays

This chapter aims to introduce the general physical principles underlaying the analysis presented in this work. For this purpose, an overview of the origin, composition and energy spectrum of cosmic rays is given in **??**, **??**, and **??** respectively. Their interactions with other matter, the physics of extensive air showers and their possible detection methods are listed in **??**.

1.1 History

A first hint at the existance of high-energy particles in the upper atmosphere was given by Hess in 1912, who found that the discharge rate of an electroscope is altitude-dependant. Millikan coined the term cosmic "rays" for these particles, as he argued the ionizing radiation must be part of the electromagnetic spectrum [**millikan1928origin**]. This was later, at least partially, falsified with the discovery of the east-west effect [**johnson1938note**]. Hess' observation however withstood the tests of time and was ultimately recognized with the Nobel prize in physics in 1936 [**nobelprize1936**]. Two years later, in 1938, Pierre Auger showed via coincidence measurements that cosmic rays in fact originate from outer space, and gave a first description of extensive air showers [**auger1939extensive**]. Another 60 years later, the Pierre Auger collaboration would adopt his experimental setup and name in their search for cosmic rays of the highest energies.

In the meantime, numerous results from different cosmic ray detectors all over the globe have helped propel the related fields of particle physics, astro physics and cosmology to new insights. Observations from cosmic ray physics serve as a valuable cross-check to the hadronic interaction models developed e.g. at CERN [**ostapchenko2007status**]. New theories modeling the final moments in the life of stars have arisen thanks to results from e.g. Kamiokande [**goldman1988implications**]. Last but not least publications by the Pierre Auger collaboration regarding the CR energy spectrum and flux help refine knowledge of our cosmic neighbourhood [**abraham2010measurement**, **aab2015searches**].

1.2 Origin

1.2.1 Acceleration

Cosmic rays whose kinetic energy far exceeds their rest energy must originate from some of the most extreme environments in space. In particular, regions with large (either in field strength or spatial extent) electromagnetic fields, where charged particles can be accelerated to significant fractions of to the speed of light, via the Lorentz force.

The question how particles are accelerated to the extremely high energies observed on earth is an active area of research. Since the discovery of cosmic rays, several candidate mechanisms and interactions have been identified and will be discussed now.

Diffusive shock acceleration (Fermi I)

Super **N**ova **R**emnants (SNR) typically feature a plasma sphere propagating outwards from the former stars core into the **I**nter **S**tellar **M**edium (ISM), in this region of plasma any magnetic field lines will be comoving, according to Alfvén's theorem [**alfven1942existence**]. First realised by Fermi, such SNR shock fronts serve as source of high-energy CRs [**fermi1949origin**].

If a low-energy particle is injected into the SNR shock front, it will eventually be reflected by the local $\vec{B}$-field. If the diffusion length within the plasma is much smaller than the spatial extent of the SNR, the shock front can be modelled as a plane, and the process is analogous to an elastic reflection against a wall. Consequently, if $\frac{d\vec{B}}{dt} = 0$, this does not cause the particle to gain any energy, espically because $W = \vec{F}_L \cdot \vec{r} \propto (\vec{v} \times \vec{B}) \cdot \vec{r} = 0$. However, because the $\vec{B}$-field is moving radially outward alongside the plasma, a net energy gain of

$$\Delta E = +\beta_{SNR} \cdot E_0 \tag{1.1}$$

arises, where $\beta_{SNR} = |\vec{v}_{SNR}| / c$ and E_0 are the velocity of the shock-front and the initial energy of the particle. From chapter 7 in [**fermi1949origin**] it follows that ionization losses within the shock front are not completely negligible. Hence a particle must have a sufficient energy such that ΔE in **??** exceeds possible ionization losses. The corresponding threshold for the primary energy above which acceleration occurs is dubbed the injection energy, and is of the order of 200 MeV for protons.

Furthermore, because typically $\beta_{SNR} \leq 0.10$ a single acceleration cycle is not enough to explain the CR energies observed on earth. Instead, multiple cycles are needed. This requires additional, focusing $\vec{B}$-fields, provided for example by the ISM, which alter the trajectory of injected particles such that they can be reflected off the shock-front again.

With each cycle, the particles rigidity $R = |\vec{p}|c / q$ increases, until its gyroradius $\rho = R/|\vec{B}|$ exceeds the spatial extent of the focusing $\vec{B}$-field and the particle escapes

into space. With an effective ejection probability p per cycle, the energy after n cycles and the expected flux w.r.t energy, $\Phi(E)$, becomes roughly

$$E(n) = E_0 \ (1 + \beta_{SNR})^n \, . \tag{1.2}$$

$$N(n) = N_0 \ (1 - p)^n$$

$$\Leftrightarrow \quad \log\left(\frac{N(n)}{N_0}\right) = n \cdot \log\left(1 - p\right)$$

$$\Leftrightarrow \quad \overset{(??)}{=} \log\left(\frac{E(n)}{E_0}\right) \frac{\log(1 - p)}{\log(1 + \beta_{SNR})}$$

$$\Leftrightarrow \quad N(E) = N_0 \cdot \left(\frac{E(n)}{E_0}\right)^{\log(1-p) \, / \, \log(1+\beta_{SNR})}$$

$$\Rightarrow \quad \Phi(E) = \frac{dN}{dE} \propto E(n)^{\alpha - 1}, \tag{1.3}$$

where $\alpha = \frac{\log(1-p)}{\log(1+\beta_{SNR})}$ in **??** is a spectral coefficient whose exact value will depend on the age of the SNR (β_{SNR} decreases with age), the injected particle (different primaries have different injection energies and ejection probabilities), as well as many other factors that are often not known a priori. It can be observed that the expected spectrum is a power law in the ranges from injection energy to a cutoff at the highest energies, which arises due to the finite lifetime of SNRs.

Results from several studies (e.g. [**aab2015searches**, **hillas2005can**, **blasi2013origin**]) hint that the presented first order Fermi acceleration mechanism is the main source of galactic CRs, extrasolar particles that originate from within the milky way, with energies ranging up to orders $O(\text{TeV})$.

Stochastic scattering acceleration (Fermi II)

Second order (or Stochastic) Fermi acceleration is the more general case of **??** and represents the original idea developed by Fermi in [**fermi1949origin**]. The underlaying principle of scattering particles off plasma clouds remains unchanged. However, if the diffusion length within the cloud exceeds its radius of curvature, the energy gain per collision instead becomes

$$\Delta E \propto + (\beta_{SNR})^2 \cdot E_0. \tag{1.4}$$

Logically, this represents a much more inefficient acceleration mechanism, but is nevertheless observed in nature under certain circumstances (c.f. [**asano2015most**]).

Centrifugal acceleration in rotating $\vec{B}$-fields

Some astrophysical objects such as pulsars or **A**ctive **G**alactic **N**uclei (AGNs) possess strong magnetic fields ranging from $1\,\text{T}$ for some AGNs [**daly2019black**] to $\approx 10\,\text{GT}$ for magnetars, a subset of pulsars with extremely high magnetic flux densities [**flowers1977evolution**].

If such objects rotate at an angular velocity Ω, which is in general nonzero, charged particles at a radial distance r from the rotation axis will undergo centrifugal acceleration. In particular, their Lorentz factor γ behaves like **??** [**rieger1999particle**].

$$\gamma := \frac{E}{m_0 c^2} = \frac{\gamma_0}{1 - \left(\frac{\Omega r}{c}\right)^2}, \tag{1.5}$$

where m_0 is the rest mass of the particle and γ_0 the prior Lorentz factor before acceleration. It follows that a test particle can in theory gain an arbitrarily high energy from this process by outspiraling towards the light cylinder surface, where $\Omega \cdot r = c$. In reality however, these processes are stopped by e.g. inverse Compton scattering at some point [**osmanov2007efficiency**]. In any case, [**rieger1999particle**] and [**osmanov2007efficiency**] conclude that values of $\gamma \approx 10^7 - 10^8$ are possible, corresponding to protons at $\approx 10\,\text{PeV} - 10\,\text{PeV}$ or iron nuclei at $\approx 500\,\text{PeV} - 5\,\text{EeV}$ energy.

Direct electrostatic acceleration

The presence of non-static $\vec{B}$-fields implies the existance of (in vacuum) comparably strong $\vec{E}$-fields and a corresponding electrical potential difference Φ across different regions within the magnetosphere. A back-of-the-envelope calculation reveals that they are (neglecting constant factors) proportional to

$$|\vec{E}| \propto \frac{\Omega\, r_0}{c} \cdot |\vec{B}|, \tag{1.6}$$

$$\Phi \propto r_0 \cdot |\vec{E}|, \tag{1.7}$$

where r_0 is the radius of the central object rotating at an angular frequency Ω. Consequently, an ion with atomic number Z can be accelerated to energies $E = Z \cdot e \cdot \Phi$, which can in some cases easily exceed 10^{20}eV [**rieger2009cosmic**].

Some caveats to this consideration need to be mentioned. Screening effects from plasma clouds surrounding the central body are expected to limit the electrical field strength, and maximum acceleration energy by extension. Additionally, losses via e.g. Bremsstrahlung have been neglected in the above calculation, limiting the maximum attainable energy in theory even further.
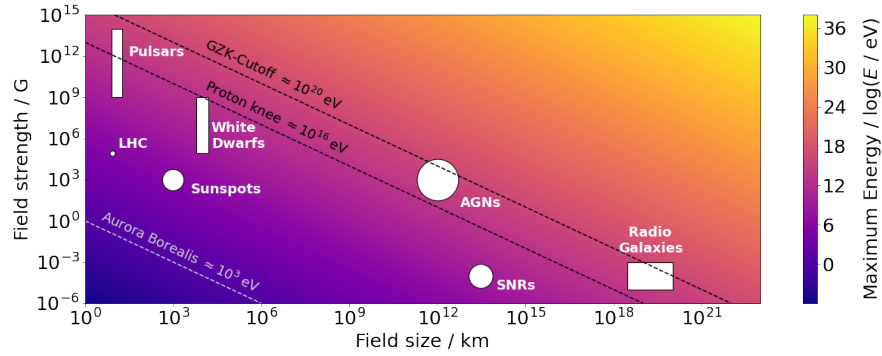
Figure 1.1: Rough estimate of field strength and size of different CR sources as well as the corresponding maximum energy estimated with **??** ($\beta = Z = 1$). Isoenergetic lines mark notable points in the energy spectrum discussed in **??**.

Other types

Several acceleration mechanisms have been discussed. A plethora of other interactions that are able to accelerate elementary particles to fantastic energies remain unmentioned, or even undiscovered, as CR physics is an active area of research. In general though the driving force behind all considered (and non-considered) acceleration mechanisms are thought to be (electro-) magnetic fields. Consequently, the maximum energy a specific CR accelerator with magnetic field $\vec{B}$ and size L moving at velocity βc can in theory provide for a particle with charge Ze is given by the Hillas formula [**hillas1984origin**]:

$$E_{\text{max}} \, [\text{PeV}] = |\vec{B}| \, [\text{µG}] \cdot L \, [\text{pc}] \cdot Z \cdot \beta \tag{1.8}$$

This allows for an elegant classification of different cosmic ray sources, in part discussed on the previous pages, according to the Hillas plot shown in **??**.

Acceleration of uncharged particles

Particles like neutrons, neutrinos or photons possess no electromagnetic charge $q = 0$. Assuming **??** holds in these cases, they should thus not appear in the CR spectrum. This is in disagreement with reality, where energies from 100 GeV up to ≈ 100 EeV have been observed [**abeysekara2018very**, **ishihara2016extremely**]. Consequently, additional interaction channels are required to explain the existance of such uncharged CRs.

High energy γ-rays in particular can be created by accelerated, charged particles via Bremsstrahlung. This occurs for example during centrifugal acceleration near pulsars or AGNs (compare **??**). Furthermore, inverse Compton scattering with a high-energy cosmic ray can imply a significant energy gain for a photon [**jones1965inverse**].

Uncharged CRs are also frequently produced in nuclear interactions, such as e.g. deeply inelastic scattering of charged CRs with the ISM. This espically contributes to the CR

photon spectrum, as high energy π^0 are often byproducts of such scattering processes. The uncharged pions then decay into two photons. Furthermore, neutrons or neutrinos can originate from interactions involving the weak force. When a proton converts to $p \rightarrow n + e^+ + \bar{\nu}_e$ during the dacy of a UHECR ion, the resulting decay products positron, neutron and electron-antineutrino inherit the parents' energy, and are thus high energy cosmic rays as well.

1.2.2 Propagation

Once a cosmic ray has been observed coming from some arrival direction (ϕ, θ), backtracking its' trajectory to an eventual origin is, ignoring external factors, in the literal sense, straight forward. It has been shown however that several effects need to be considered for an accurate treatment of CR propagation.

For uncharged CRs (γ, n), this task is simple. Such particles are not deflected by cosmic $\vec{E}$ and $\vec{B}$-fields. Possible interactions either demand the destruction of the particle (pair production, weak decay), or occur close to the source (e.g. Compton scattering), in which case the observed arrival direction will still be coincident with the actual source [**fermi201398**]. Gravitational lensing effects in some cases alter the trajectory of extragalactic photons. Such phenomena (if present in the first place) are however well understood in the scope of general relativity, and can be corrected for [**bartelmann2010gravitational**, **bartelmann2001weak**].

Intergalactic propagation & transport equation

Contrary, charged particles ($e^\pm$, p, ions) propagate along non-trivial paths within galaxies due to deflections from solar- and galactic EM-fields. While the galactic field is coherent over large scales, numerous irregular magnetic domains, seeded in part by individual stars complicate CR propagation to essentially a three-dimensional random walk [**haverkorn2015magnetic**]. It is thus challenging to pinpoint the origin of a charged cosmic ray.

Nevertheless, related queries, such as for example the question whether or not a particle of given energy is likely to be of extragalactic origin can be answered by examining the distribution of cosmic rays within a region of spacetime. The behaviour of a population of n_i particles of type i can be approximately recreated via the below transport equation:

$$\frac{\partial n_i}{\partial t} = \underbrace{Q_i}_{\text{Source}} + \underbrace{\nabla D_i\left(\nabla n_i\right)}_{\text{Diffusion}} - \underbrace{\frac{\partial k_i(E)}{\partial E}}_{\text{Energy}} - \underbrace{\left(\frac{n_i}{\tau_{\text{spal.},i}} - \sum_{j>i}\frac{n_j\, p_{ij}}{\tau_{\text{spal.},j}}\right)}_{\text{Spallation}} - \underbrace{\left(\frac{n_i}{\tau_{\text{rad.},i}} - \sum_{j>i}\frac{n_j\, d_{ij}}{\tau_{\text{rad.},j}}\right)}_{\text{Weak decay}}$$

- **Source Q_i :**

The source term is responsible for the creation of CR particles (of type i). The exact form of Q_i will depend on the considered creation process. For example, the near instantaneous creation of n_γ photons in a **Gamma-Ray Burst** (GRB) at time t_0 and location $\vec{r}_0$ can be modelled like $Q_\gamma = n_\gamma \, \delta(\vec{r} - \vec{r}_0) \, \delta(t - t_0)$.

- **Diffusion** $\nabla D_i \, (\nabla n_i)$:

  The random walk mentioned above is accounted for in the diffusion term, which takes a similar form to the Stokes-Einstein equation. The diffusion coefficient(s) D_i in general take a tensor form due to anisotropic diffusion in different directions. Furthermore, D_i is different for each particle type, as the deflecting EM-fields couple to the respective charges q_i, which need not be equal in principle.

- **Energy loss** $\partial k_i(E) \, / \, \partial E$:

  During propagation, a cosmic ray can interact with the ISM, and lose energy in the process. If this happens often enough, the CR is eventually thermalized and does not contribute to the population i any longer. Different interaction channels for different CR types i require different loss models $k_i(E)$ for each type.

- **Spallation** $\left(n_i \, / \, \tau_{\mathrm{spal.}, i} - \sum n_j \, p_{ij} \, / \, \tau_{\mathrm{spal.}, j} \right)$:

  Nuclear spallation describes the process of violent disintegration of a target nucleus upon being struck by an energetic projectile. The resulting fragments can retain energies up to the projectiles energy. The spallation term in the transport equation considers both the destruction (first term), as well as creation (second term) of CRs i from heavier types j. It is assumed that spallation from type $j \rightarrow i$ occurs at a constant probability of p_{ij} in a characteristic time frame $\tau_{\mathrm{spal.}, j}$.
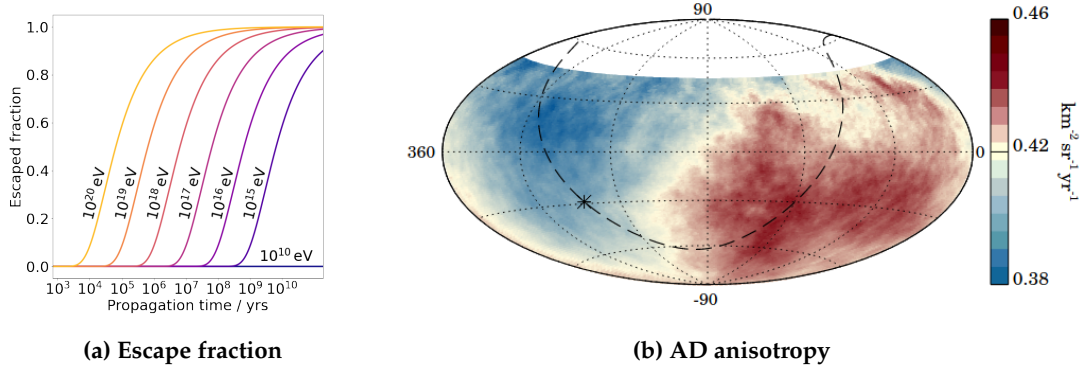
- **Weak decay** $\left(n_i \, / \, \tau_{\mathrm{rad.}, i} - \sum n_j \, d_{ij} \, / \, \tau_{\mathrm{rad.}, j} \right)$:

  If a particle j is weakly unstable ($\tau_{\mathrm{rad.}, i} < \infty$) there is a nonzero chance d_{ij} it decays into a daughter nuclei of some type i during propagation. The decay term reflects this and describes both decay from heavier and decay into lighter nuclei.

Insights to the physical implications of this parametrization can be gathered from a simplified example. Consider the case of a galaxy with height $2H$ and width W. It is $H \ll W$, and thus only diffusion along the $\pm z$-direction will be examined. Considering n_0 protons located at $z = 0$ initially, and ignoring interactions with the ISM, the transport equation reduces to the first two terms, with $D = (0, 0, D_z)^{\mathrm{T}}$ and $Q = n_0 \, \delta(z) \, \delta(t_0)$.

It can quickly be verified that a solution to the transport equation in this case is given by a normal distribution with mean $\mu = 0$ and standard deviation $\sigma = \sqrt{2 D_z t}$. The diffusion coefficient D_z is a measure of how quickly the population spreads out (along the $\pm z$-direction). According to [**skilling1970diffusion**], D_z can be parametrized via the particles energy E_p, and characteristics of the present $\vec{B}$-fields.

$$D_z = \frac{1}{3} \gamma \cdot \lambda = \frac{1}{3} \frac{E_p}{m_p \, c^2} \cdot \frac{|\vec{B}| \cdot \langle L_{\vec{B}} \rangle}{\sqrt{\mu_0 \, \rho_{\mathrm{ISM}}}}, \tag{1.9}$$

(a) Escape fraction

(b) AD anisotropy

Figure 1.2: (a) $r_{\text{esc.}}(t)$ according to **??** for protons of different energies.
(b) Dipole in the arrival direction of CRs with $E > 8\,\text{EeV}$. Image copied from [**pierre2017observation**].

where $\langle L_{\vec{B}} \rangle$ is the characteristic length scale of deflecting $\vec{B}$-fields, μ_0 and ρ_{ISM} are the magnetic vacuum permeability and density of the interstellar medium respectively. After some time t, a fraction $r_{\text{esc.}}(t)$ of particles will have a z-coordinate $|z| > H$, and exit the disc consequently. In reality, this is not equivalent to the particle leaving the galaxy, as large-scale halo structures extend above and below the visible disc [**searle1978compositions**]. These halos are ignored here. $r_{\text{esc.}}(t)$ can thus be calculated according to **??**. For some selected energies, a plot of the escaping ratio over time is offered in **??**.

$$r_{\text{esc.}}(t) := 1 - \int_{-H}^{H} \frac{n(z,t)}{n_0} \, \text{d}z \tag{1.10}$$

It can be concluded that low energy CRs do not travel outside their host galaxy within reasonable timeframes. Meanwhile, **U**ltra **H**igh **E**nergy CRs (UHECR, $E > 10^{18}$ eV) escape swiftly on ballistic trajectories and can (and often do) have an extragalactic origin, not last also due to the limited energies that CR sources in the milky way can provide (compare **??**).

This observation is consistent with a dipole in the **A**rrival **D**irection (AD) of UHECRs observed by the Pierre Auger observatory. The dipole points roughly in the opposite direction of the galactic core, marked with an asterisk in **??**.

Extragalactic propagation & GZK-Cutoff

In the last paragraph the (likely) extragalactic origin of UHECRs was discussed. Such particles must traverse millions of lightyears of extragalactic space before inducing a large air shower on earth. As the energy of these primaries increases above the **G**reisen-**Z**atsepin-**K**usmin threshold (GZK), their propagation through space is thought to be severely impeded. At energies above $\approx 10^{20}$ eV the **C**osmic **M**icrowave **B**ackground

(CMB) consisting of photons in the microwave rage are blueshifted to energies $E_\gamma >$ 300 MeV. A proton with the corresponding energy can thus absorb such CMB photons and convert to its' excited spin state, the Δ^+-baryon. The Δ^+-baryon decays nearly instantanouely to (for example) its' ground state again, by radiating away a π^0 [**PDG**] and losing energy in the process [**PDG**].

The mean free path of this interaction, also labelled GZK horizon is both energy- and primary-dependant. For 75 EeV protons, it is $\approx$ 100 Mpc. Cosmic rays exceeding the GZK threshold should ergo not be observed from faraway sources, and an overall reduction in flux at these energies should be recorded.

Indeed, results published by the Auger collaboration (see **??**) are consistent with this assumption. Whether or not the GZK-supression is the main cause for this hard spectrum at the highest energies remains unclear for now, but shall hopefully be answered with the ongoing AugerPrime upgrade of Pierre Auger observatory.
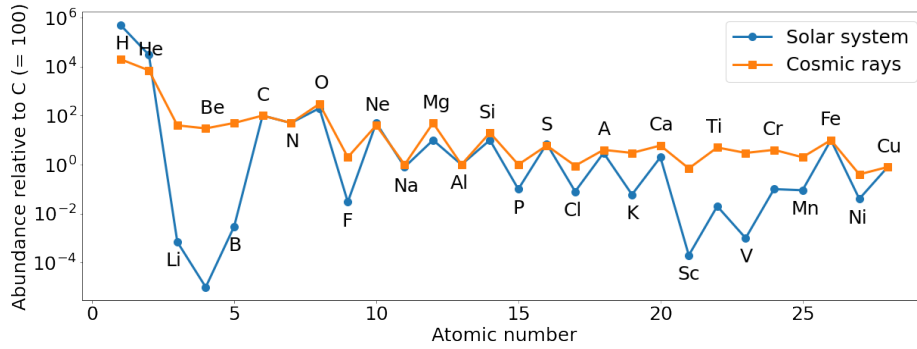
1.2.3 Composition

The composition of CRs largely mirror the relative abundancies of elements in the universe with some noteable exceptions shown in **??**. Elements like beryllium (Be) or vanadium (V) are atypical products of supernovae and thus not as common as e.g. oxygen (O) [**gamezo2005three**, **cowan2004r**] in the solar system. This leads to a dip in the corresponding abundancy spectrum. The same dip is not observed in CR primary abundancies. While it is a priori existant upon creation of cosmic rays, but gradually gets "filled up" via e.g. spallation processes during their propagation until an equilibrium state is reached.

This equilibrium state depends sensitively on the characteristic age of cosmic rays, i.e. the mean travel time until a particle escapes the galaxy. Measuring CR composition hence enables the estimation of this parameter. Such an analysis is conducted in [**garcia1977age**], where it is found that the observed abundancies are consistent with a characteristic age of 1.7×10^7 yr for such high energy particles.

Contrary, hydrogen (H) and helium (He) are underrepresented (w.r.t their natural abundancy in the solar system) in cosmic ray particles. This is likely due to the comparably high ionization energy of both elements, which leads to less readily available hydrogen/helium ions. Since the acceleration mechanisms discussed in **??** all couple to the net charge q of a particle, unionized hydrogen and helium are not accelerated [**wang2002measurement**].

1.3 Energy spectrum

It has been discussed in **??** that the expected CR flux w.r.t energy for supernova remnants is a powerlaw in the rough range of 200 MeV $< E \lesssim$ 100 TeV. Observations by various experiments extend this result to even higher energies. Their combined results are shown in **??**. However, while the general assumption of a powerlaw $\Phi(E) \propto E^\alpha$ holds

Figure 1.3: Composition expressed as abundancy relative to carbon for different sources. The ragged, alternating structure stems from an increased stability of nuclei with an even amount of protons (c.f. for example [**kirson2008mutual**]). Data from [**gaisser2016cosmic**]

over a large range of energies, kinks and other feature in the spectrum indicate that the spectral index α is not uniform, and instead a function of energy. The approximate form of $\alpha(E)$ will be discussed in the following by examining several key regions of the energy spectrum.

1.3.1 Proton knee $E \approx 10^{15}\,\mathrm{eV}$

Below an energy of $\approx 1\,\mathrm{PeV} = 10^6\,\mathrm{eV}$, it is $\alpha(E) \approx 2.7$, while above a spectral index of $\alpha(E) \approx 3.0$ is found [**gaisser2016cosmic**]. This softening of the spectrum (i.e. fewer particles of higher energy), can be attributed to several effects, some of which could not be falsified by measurements yet.

- **Dark matter channel** (partially falsified)

  Weakly **I**nteractive **M**assive **P**articles (WIMPs) are a popular candidate for **D**ark **M**atter (DM), as they correctly estimate the cosmological evolution of the universe [**klypin1993structure**]. A WIMP with a sufficiently high mass could explain the kink in the above spectrum. CRs with an energy exceeding the rest mass of the WIMP could in theory produce DM in deeply-inelastic scattering processes. The degree of steepening in the spectrum is a measure for how readily the process $X \to \mathrm{WIMP} + Y$ occurs, and can be used to estimate the corresponding cross sections. Most theories involving WIMP creation can be excluded, since detectors at earthbound particle accelerators should have observed DM production at the observed steepening from 2.7 to 3.0 [**donato2009constraints**].

- **Escape during propagation**

  While the analysis in **??** concludes that the escape time for $10^{15}\,\mathrm{eV}$ protons to leave their host galaxy is at least of the order $\approx 10^8\mathrm{yr}$ (compare **??**), the calculations leading to this result are extremely simplified. If a more accurate treatment finds that particles with rigidities corresponding to the relevant energies are no longer
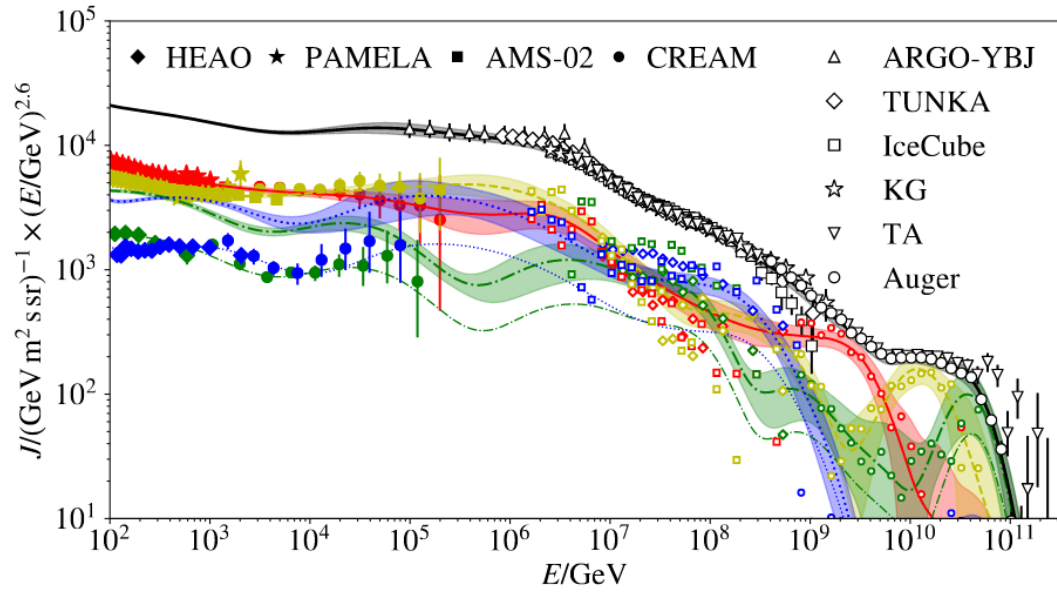
Figure 1.4: Measurements of the cosmic ray flux, multiplied by a factor $E^{2.6}$ for all types (black), and broken down by primary. Shown are protons (red), helium (yellow), oxygen (green) and iron (blue). Plot adopted from [**dembinski2017data**].

confined by galactic magnetic fields, the kink could originate from particles leaving the milky way and not contributing to the flux observed on earth any longer.

- **Limited source energy**

1.3.2 Iron knee $E \approx 10^{17}$ eV

sughlksghksulhg

1.3.3 Ankle $E \approx 10^{18}$ eV

ajshgkljghkfgkldfyg

1.3.4 Cutoff $E \approx 10^{20}$ eV

1.4 Extensive air showers